

## Chapter 7

# Site Specific Sequestering and Stabilization of Charge in Peptides by Supramolecular Adduct Formation with 18-Crown-6 Ether via Electrospray Ionization

Portions published previously in: Julian R. R.; Beauchamp J. L. *Int. J. Mass Spectrom.* **2001**, *210*, 613-623.

### 7.1 Introduction

The discovery of crown ethers has lead to many solution phase applications.<sup>1</sup> However, until recently, the applications to gas phase chemistry have been limited in comparison.<sup>2,3</sup> Crown ethers are capable of forming supramolecular assemblies in the gas phase, and with the introduction of electrospray ionization (ESI), the means for easily characterizing these species is now available. 18-Crown-6 ether (18C6) binds cationic species. These adducts have been studied in both solution<sup>4,5</sup> and the gas phase.<sup>6-9</sup> The binding affinity of 18C6 is high for metal cations (Table 7.1).<sup>6</sup> 18C6 also forms stable gas phase adducts with amines.<sup>7</sup> The selectivity of crown ethers is determined by the cavity

size, which allows 18C6 to bind primary amines better than other candidate crown ethers.<sup>8,9</sup>

**Table 7.1 Experimental<sup>a</sup> and Computational<sup>b</sup>  
Bond dissociation energy for 18C6 complexes**

Molecule	Bond Dissociation Energy (kJ/mol)
$[(\text{Methylamine}+\text{H})\text{CE}]^+$	182 <sup>b</sup>
$[(\text{Lys}+\text{H})\text{CE}]^{+\text{c}}$	150 <sup>b</sup>
$[(\text{Arg}+\text{H})\text{CE}]^{+\text{c}}$	133 <sup>b</sup>
$[(\text{His}+\text{H})\text{CE}]^{+\text{c}}$	127 <sup>b</sup>
$[\text{Na}\cdot\text{CE}]^+$	300 <sup>a</sup>
$[\text{K}\cdot\text{CE}]^+$	235 <sup>a</sup>
$[\text{Rb}\cdot\text{CE}]^+$	192 <sup>a</sup>
$[\text{Cs}\cdot\text{CE}]^+$	170 <sup>a</sup>

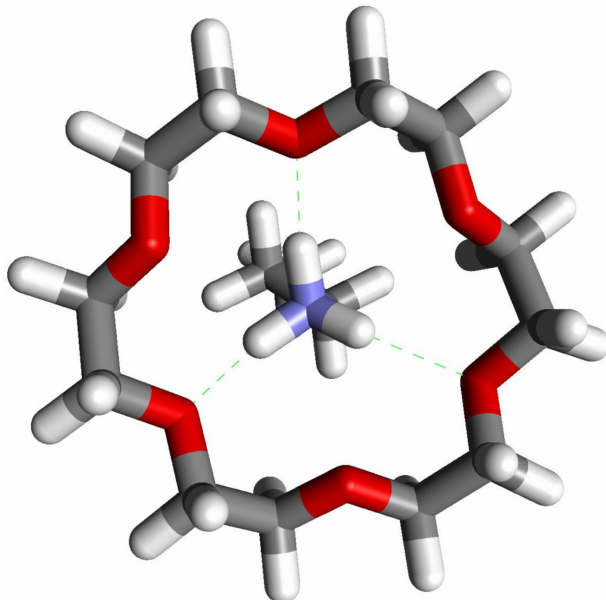
<sup>a</sup> taken from reference 6

<sup>b</sup> calculated with PM3 relative to separated monomers

<sup>c</sup> in each case the CE was attached to the side chain

Lysine is a basic amino acid that plays an important role in the solvation, structure, and activity of proteins.<sup>10</sup> The side chain of lysine terminates in a primary amine. It is possible to form a strong, hydrogen bound complex between 18C6 and protonated lysine. As a model for this, structure 7.1 depicts the noncovalent association between protonated butylamine and 18C6. Alternating oxygens of 18C6 are coplanar and serve as hydrogen bond acceptors for the protonated primary amine. The location and orientation of these three oxygens is optimal for primary amines (average N—O distance 3.1 Å) and lends specificity to the binding. The bond dissociation for this interaction is 182 kJ/mol as indicated by PM3 calculations (Table 7.1). The interaction depicted in 7.1 has been applied successfully in our laboratory to study the mechanism of gas phase H/D exchange in small protonated peptides, specifically a series of glycine oligomers.<sup>11</sup> These

experiments derived advantage from the ability of 18C6 to sequester protons attached to the protonated N-terminus and inhibit their interaction with deuterated reagents that normally would have effected rapid H/D exchange.



## 7.1

In the present work, the interaction between lysine and 18C6 is studied with various lysine derivatives to establish the preferred binding site. The ability of 18C6 to form highly charged multiple adducts is investigated through polylysine peptides. An original objective of this study was to use the molecular recognition capabilities of 18C6 to count lysine residues in peptides of unknown sequence. It is shown, however, that complications result from competitive complexation by the protonated side chains of histidine, arginine, and particularly the n-terminus of peptides that do not contain lysine. Nevertheless, 18C6 is shown to be a sensitive chemical probe of molecular structure, and experiments with cytochrome-c and bovine pancreatic trypsin inhibitor (BPTI) suggest that 18C6 can provide information relating to surface functional groups of folded proteins. The binding of 18C6 to peptides and proteins dramatically alters both the ion

abundance and the observed charge state distribution. This charge stabilization is useful because it allows for the facile detection of species that are normally difficult to detect with ESI. The interaction of <sup>18</sup>C6 with molecular ions sheds further light on the mechanism of ESI, which remains poorly understood.<sup>12</sup> The results are best rationalized in accordance with the ion evaporation mechanism originally proposed by Iribarne and Thomson.<sup>13</sup>

## 7.2 Experimental Methodology

All spectra were obtained using a Finnigan LCQ ion trap quadrupole mass spectrometer without modification. The critical instrument settings that yield adduct formation include capillary voltage 14.12V, capillary temperature 200°C, and tube lens offset -39V. Higher capillary temperatures dissociate the <sup>18</sup>C6 complexes. The tube lens offset controls the acceleration of ions as they leave the capillary region. The tube lens voltage is minimized to avoid collisions with the He buffer gas. Soft sampling is crucial for the detection of these noncovalent complexes.

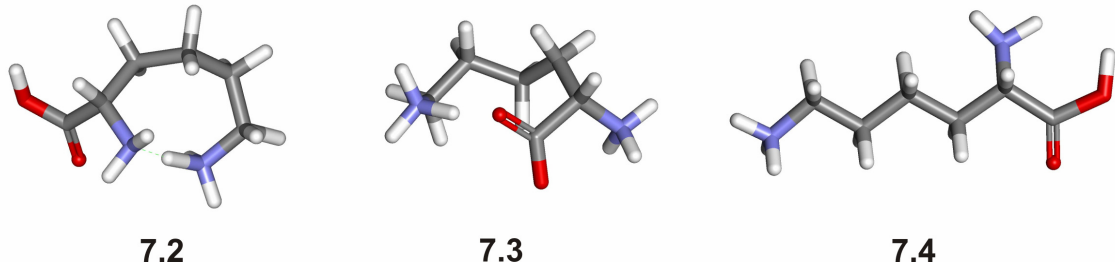
Sample concentrations were typically kept in the ~10 to 100 μM range for all species of interest, unless otherwise noted. All samples were electrosprayed in a mixture of 80:20 methanol/water. <sup>18</sup>C6 was added to the sample and electrosprayed with the analyte in order to observe adducts. Samples were electrosprayed with a flow of 3-5 μL/min from a 500 μL Hamilton syringe for optimal signal. Silica tubing with an inner diameter of .005 in was used as the electrospray tip. No acid was added to any of the samples, unless otherwise noted. Acid has a tendency to decompose <sup>18</sup>C6 under electrospray conditions. All chemicals unless otherwise noted were purchased from

Sigma or Aldrich and used without further purification. The cytochrome-c used in this study was taken from horse heart. KK-methyl ester was synthesized by dissolving KK in methanol with 1% H<sub>2</sub>SO<sub>4</sub> and heating to 60°C for one hour. The yield was ~85 percent as determined by mass spectrometry.

All semi-empirical calculations were performed with the HyperChem 5.1 Professional Suite. Candidate structures were identified with molecular mechanics using Cerius<sup>2</sup> version 4.0 by Molecular Simulations Inc. with the Dreiding 2.21<sup>14</sup> force field. Molecular volumes are based on a smoothed Van der Waals radius and were calculated with Cerius<sup>2</sup>. Jaguar 4.0, Schrodinger, Inc., Portland, Oregon, 2000 was used to perform all density functional theory (DFT) calculations at the B3LYP level with the 6-31G\*\* basis set.

### 7.3 Results and Discussion

**Lysine and Lysine Derivatives.** A mixture of lysine and lysine methyl ester (MeLys) was electrosprayed with the addition of 18C6. The observed mass spectrum is shown in Figure 7.1a. The complex [Lys+18C6+H]<sup>+</sup> is formed and is singly charged. The spectrum shows that only a single 18C6 adds to lysine. This is not the case for MeLys, where there is a significant doubly charged double adduct peak corresponding to [MeLys+2(18C6)+2H]<sup>2+</sup>. The C-terminus of MeLys is methylated, precluding deprotonation. The presence of an adduct with two 18C6 ethers attached in the case of MeLys contrasts with the observation that lysine attaches only a single 18C6. The difference in behavior between these species can be attributed to a stable molecular conformation that is only available to lysine.



DFT calculations were performed on several possible conformations of protonated lysine (shown as structures **7.2-7.4**). The structures were fully minimized at the B3LYP/6-31G\*\* level. The high proton affinity of lysine (238 kcal/mol) relative to butylamine (220.2 kcal/mol) can be attributed to the favorable intramolecular hydrogen bond<sup>15</sup> formed in structure **7.2**, which must be broken to attach 18C6. Just 3 kcal/mol in energy above **7.2** is the salt bridge structure **7.3**, with the carboxylate between the two protonated amine sites. Structure **7.3** can only bind 18C6 at the n-terminus without significantly disrupting the favorable electrostatic interaction in the salt bridge. 18C6 can attach to the side chain in structure **7.4**, which is 16.1 kcal/mol higher in energy than **7.2**. Thus it is likely that 18C6 will attach preferentially to the n-terminus of lysine to preserve the 13 kcal/mol stabilization afforded by the salt bridge structure. Doubly protonated MeLys can attach two 18C6 ethers in a conformation similar to that shown in **7.4** because it is incapable of forming a salt bridge structure similar to structure **7.3**.

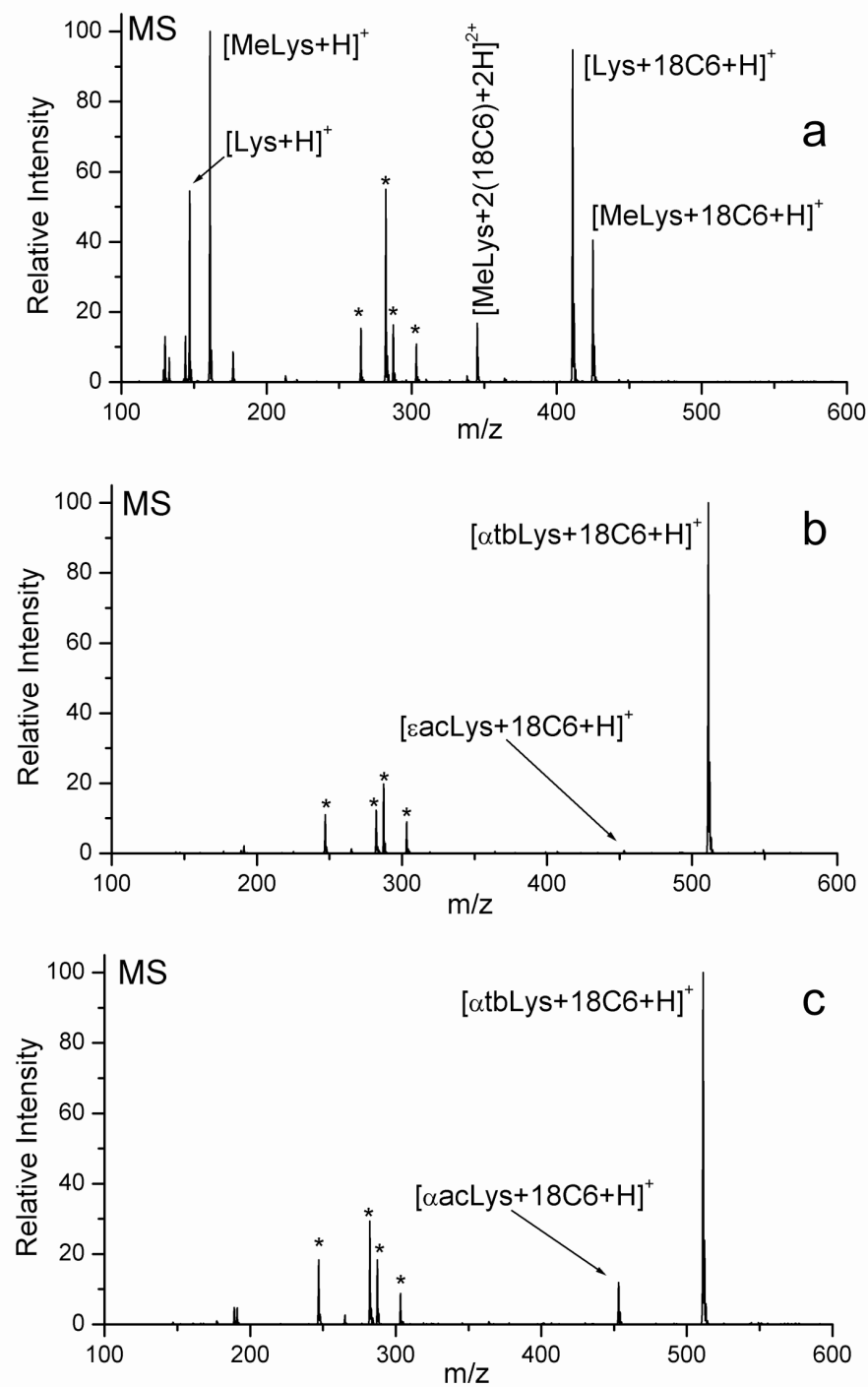
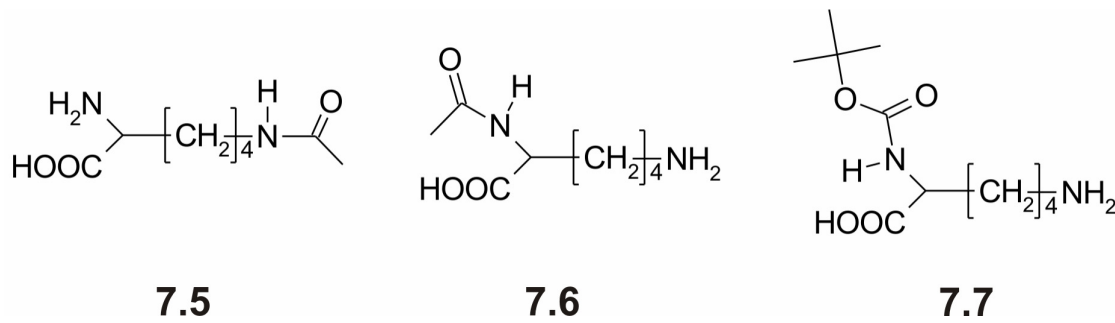


**Figure 7.1** (a) Mass spectrum of equimolar mixture of Lys and MeLys with 18C6 showing the difference in binding between these two similar species. The preference for binding to the side chain of lysine is shown by comparison of the competitive binding

between (b) 18C6 with equimolar amounts of  $\epsilon$ -n-acetyl lysine and  $\alpha$ -n-tertbutoxycarbonyl lysine, and (c) equimolar  $\alpha$ -n-acetyl lysine and  $\alpha$ -n-tertbutoxycarbonyl lysine with 18C6. \* indicates peaks corresponding to other 18C6 peaks.

The competitive binding of 18C6 to the n-terminus and the alkyl-ammonium side chain of lysine were probed with lysine derivatives **7.5-7.7**. The results are shown in Figure 7.1b and Figure 7.1c. The effect of blocking the side chain in **7.5** was compared to blocking the N-terminus in **7.6** and **7.7**. The direct comparison of N-acetylated species is not possible due to their identical mass, and therefore the binding affinities were compared relative to **7.7**. In each case, equimolar mixtures of the lysine derivatives were electrosprayed with 18C6. The intensity of the 18C6 complex with **7.5** is 15 times smaller than that for 18C6 complexed with **7.6**. This suggests that 18C6 has a strong preference for binding to the side chain of lysine when there is no possibility of salt bridge formation.



**Arginine and Histidine.** The side chains of lysine, arginine, and histidine all contain basic sites that are protonated at biological pH and can therefore interact with 18C6. To

examine the binding affinity of 18C6 for each of these side chains a solution of 50  $\mu\text{M}$  each of imidazole, guanidine, and n-butyl amine was electrosprayed with 10  $\mu\text{M}$  18C6. The spectrum is shown in Figure 7.2a. It is observed that  $[\text{nbutylamine}+\text{18C6}+\text{H}]^+$  completely dominates the spectrum, with 3.5% relative intensity for the guanidinium adduct and 1% for the imidazole ring adduct. This result demonstrates the preference of 18C6 for binding to a protonated primary amine, especially considering that n-butyl amine has the lowest proton affinity<sup>16</sup> of these three molecules (Table 7.2). In a similar experiment 50  $\mu\text{M}$  n-butyl amine and alanine were electrosprayed with 10  $\mu\text{M}$  18C6. Again the results (Figure 7.2b) show that 18C6 has a definite preference for the terminal alkyl amine over the n-terminus.

**Table 7.2 Molecular Volume and Proton Affinity of Various Species**

Species	Molecular Volume ( $\text{\AA}^3$ )	Proton Affinity (kJ/mol) <sup>a</sup>
18C6	263.32	967 <sup>b</sup>
$\text{NH}_4^+$	25.84	--
KK	--	1012 <sup>c</sup>
$[\text{KK}+\text{H}]^+$	--	842 <sup>c</sup>
$[\text{KK}+2\text{H}]^{2+}$	--	591 <sup>c</sup>
KKKK	--	1079 <sup>c</sup>
$[\text{KKKK}+\text{H}]^+$	--	967 <sup>c</sup>
$[\text{KKKK}+2\text{H}]^{2+}$	--	760 <sup>c</sup>
$[\text{KKKK}+3\text{H}]^{3+}$	--	680 <sup>c</sup>
Lys	--	996 <sup>b,c</sup>
$[\text{Lys}+\text{H}]^+$	--	693 <sup>c</sup>
MeLys	--	1004 <sup>c</sup>
$[\text{MeLys}+\text{H}]^+$	--	696 <sup>c</sup>
Methanol	--	754.3 <sup>b</sup>
Guanidine	--	986.3 <sup>b</sup>
n-butyl amine	--	921.5 <sup>b</sup>
Imidazole	--	942.8 <sup>b</sup>
Glycine	--	886.5 <sup>b</sup>
Alanine	--	901.6 <sup>b</sup>

<sup>a</sup> calculated values adjusted to match experimental PA of lysine.

<sup>b</sup> taken from reference 23.

<sup>c</sup> calculated with PM3 using the experimental heat of formation for  $\text{H}^+$ .

**Proline, Glycine, and Alanine.** Protonated proline does not form an observable adduct with 18C6 (spectrum not shown). Thus only a peptide with a primary amine n-terminus can bind 18C6 at that position. In the absence of basic residues, there is an immediate benefit that results from the ability of 18C6 to bind to a protonated n-terminus. Glycine and Alanine are two amino acids that are difficult to electrospray, particularly in the absence of acid. This is most likely due to the low proton affinities of these amino acids. With the addition of 18C6, glycine and alanine are detected easily by ESI mass spectrometry in the absence of acid (as seen in Figure 7.2c). The isolated charged species can be obtained via mild CID. As discussed further below this observed charge stabilization in transferring ions from solution to the gas phase appears consistent with the ion evaporation model<sup>13</sup> for ESI.

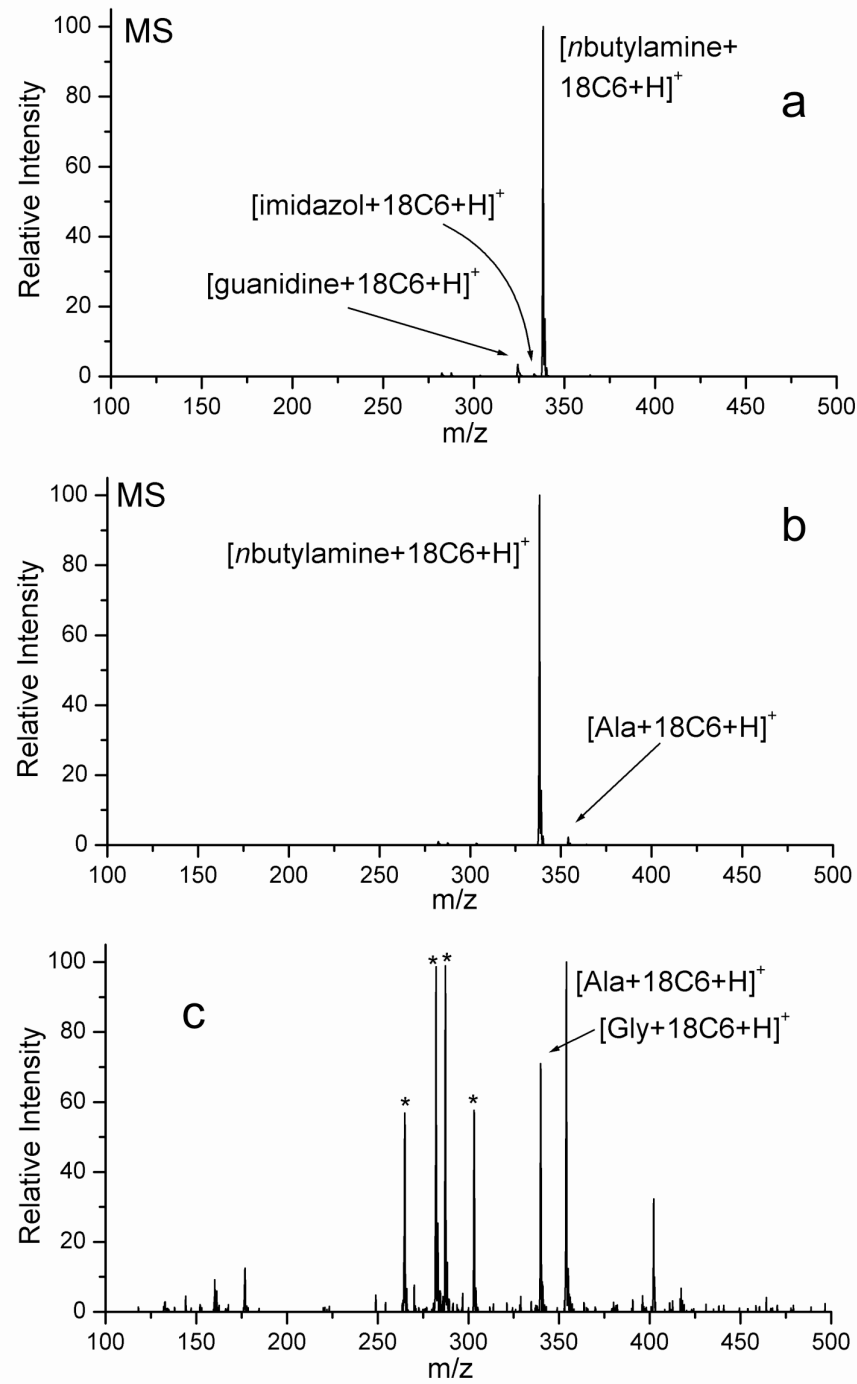


**Figure 7.2** (a) Equimolar mixture of n-butyl amine, imidazole, and guanidine with  $^{18}\text{C}_6$ . These functional groups represent the side chains of lysine, histidine, and arginine respectively and effectively approximate the competitive binding between these amino acids without interference from the N-terminus. (b) Spectra of equimolar mixture of n-

butyl amine and alanine in which the N-terminus is shown to be much less favored than a terminal alkyl amine. (c) In the absence of alkyl amines, glycine and alanine are easily detected by complexation with 18C6 in the absence of acid.

**Polylysines.** The di-peptide KK was electrosprayed with and without 18C6. The results are shown in Figures 7.3a and 7.3b, respectively. KK is singly charged when electrosprayed under normal conditions, even with the addition of 0.1% acetic acid. With the addition of 18C6, the primary peak is  $[KK+2(18C6)+2H]^{2+}$ . There are additional minor peaks corresponding to one 18C6 adduct (singly and doubly charged). The +2 charge state that is absent in the spectrum of KK alone becomes the primary peak with the addition of 18C6. In a similar result, methyl-ester dilysine (Me-KK) attaches two 18C6 ethers to a doubly charged cation (spectra not shown). This supports the evidence given above suggesting that the 18C6 attaches to the side chain of lysine. KK is unable to form the salt bridge structure found in lysine, therefore the spectrum of Me-KK with 18C6 present yields results essentially identical to those for KK. This again points to the fact that lysine itself is a special case.

The tetra-peptide KKKK was electrosprayed with and without 18C6 (Figure 7.3c and Figure 7.3d). The peptide is primarily doubly charged under normal electrospray conditions. In the presence of 18C6,  $[KKKK+4(18C6)+4H]^{4+}$  is formed. The complex is quadruply charged as seen in the inset high resolution scan in Figure 7.3d. The side chains are flexible enough to accommodate multiple crown ethers complexed to adjacent lysines. This is illustrated by the PM5 structure 7.8 for the tetra-adduct of KKKK.

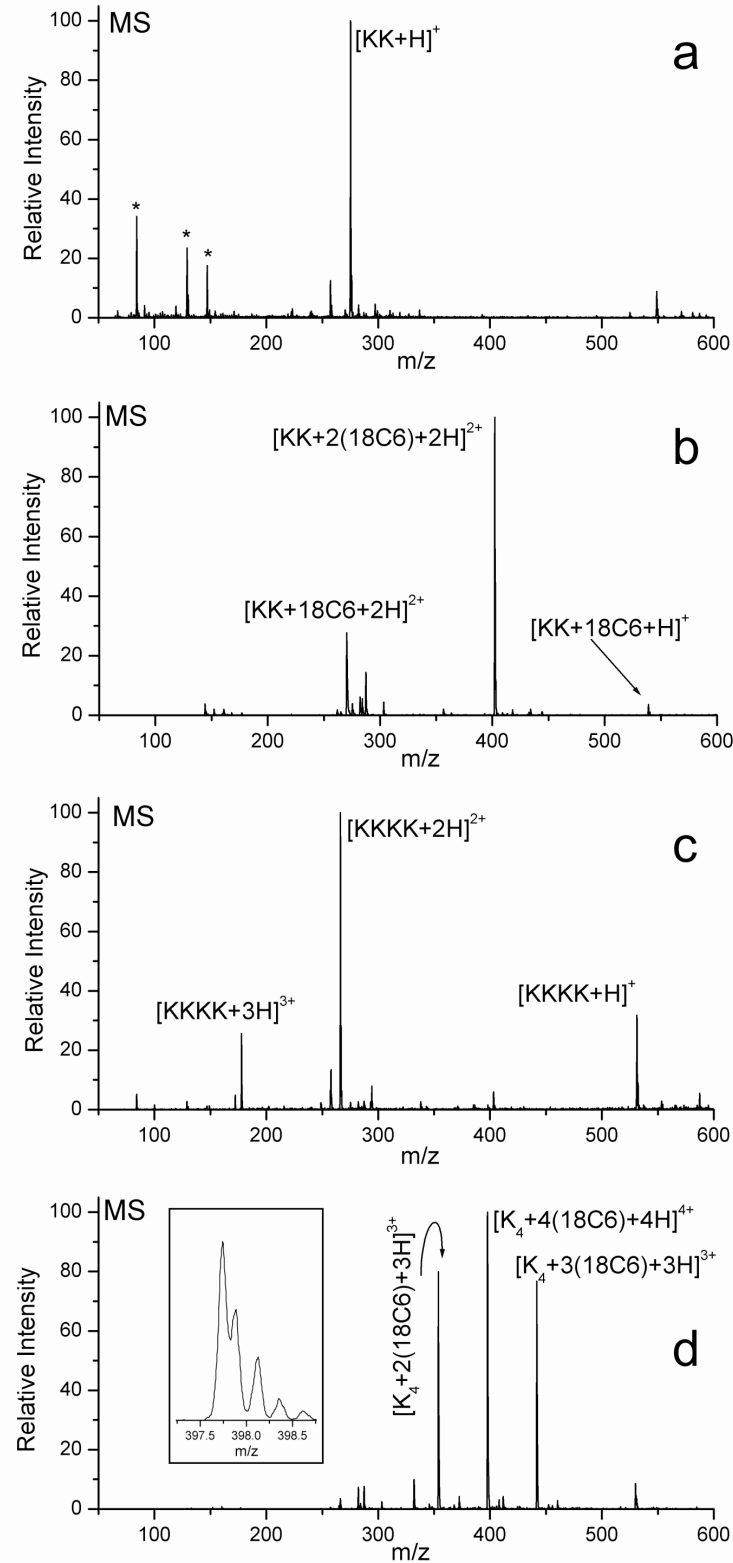
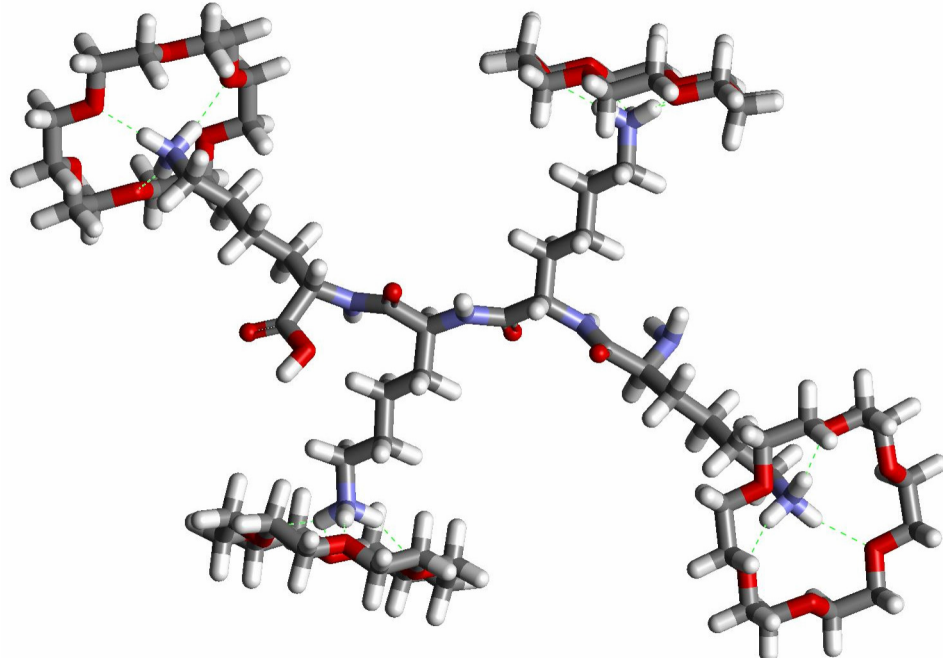


**Figure 7.3** Caption on following page.

**Figure 7.3** Polylysine spectrum illustrating the charge stabilization between (a), the ESI spectrum of KK with acid under normal ESI conditions, and (b) ESI of KK with 18C6 in the absence of acid. This result is more dramatically repeated in comparison of (c) typical ESI spectrum of KKKK with (d), the ESI spectrum of KKKK with 18C6 (inlaid portion is zoomscan of peak near 398). Notice the increase in charge state for both molecules and the 1:1 Lys to 18C6 complexation. \* indicate lysine fragments.



7.8

**Small Model Peptides.** Two peptides containing both Arg and Lys were examined. The dipeptide RK is both singly (59%) and doubly (41%) charged under normal electrospray conditions. The spectrum of RK mixed with 18C6 is shown in Figure 7.4a. The primary peak is a doubly charged species corresponding to  $[RK+18C6+2H]^{2+}$ . A typical electrospray spectrum for Tuftsin (TKPR) shows that this peptide prefers to be

singly (84%) charged. As shown in Figure 7.4b, it becomes primarily doubly charged with the addition of 18C6. The most abundant crown ether adduct for TKPR with 18C6 is  $[TKPR+18C6+2H]^{2+}$ .

The peptide PHPFHFVTK (referred to as Turn) contains one lysine, two histidines, and proline at the n-terminal position. The spectrum of Turn in Figure 7.4c was taken under normal electrospray conditions and demonstrates a preference for the doubly charged state. When 18C6 is added (Figure 7.4d), the charge state increases to +3 and there is primarily one crown ether adduct, i.e.,  $[Turn+18C6+3H]^{3+}$ . The singly charged peptide does not have a corresponding 18C6 adduct peak, suggesting that the labile proton preferentially resides on one of the histidines. The doubly charged peptide attaches only one 18C6, suggesting that the charges reside on opposite ends of the molecule with one proton on the c-terminal lysine and the other on the histidine adjacent to the n-terminus. The addition of a third proton likely occurs on the remaining histidine, and can be accompanied by attachment of a second 18C6, leading to the peak corresponding to a double 18C6 adduct.

The results suggest that for biologically relevant multifunctional peptides, 18C6 has a strong but not exclusive preference for binding to the side chain of lysine. As an alternative binding site, the peptide n-terminus is significantly less basic and more sterically constrained than the side chain of lysine.<sup>17</sup> Arginine and histidine are more basic than lysine but lack the stronger specific binding of 18C6 to protonated primary amines. In small peptides 18C6 can bind to adjacent lysines, and there is a one to one correlation between the number of attached 18C6 ethers and lysine residues in what is usually the most intense peak in the spectrum.

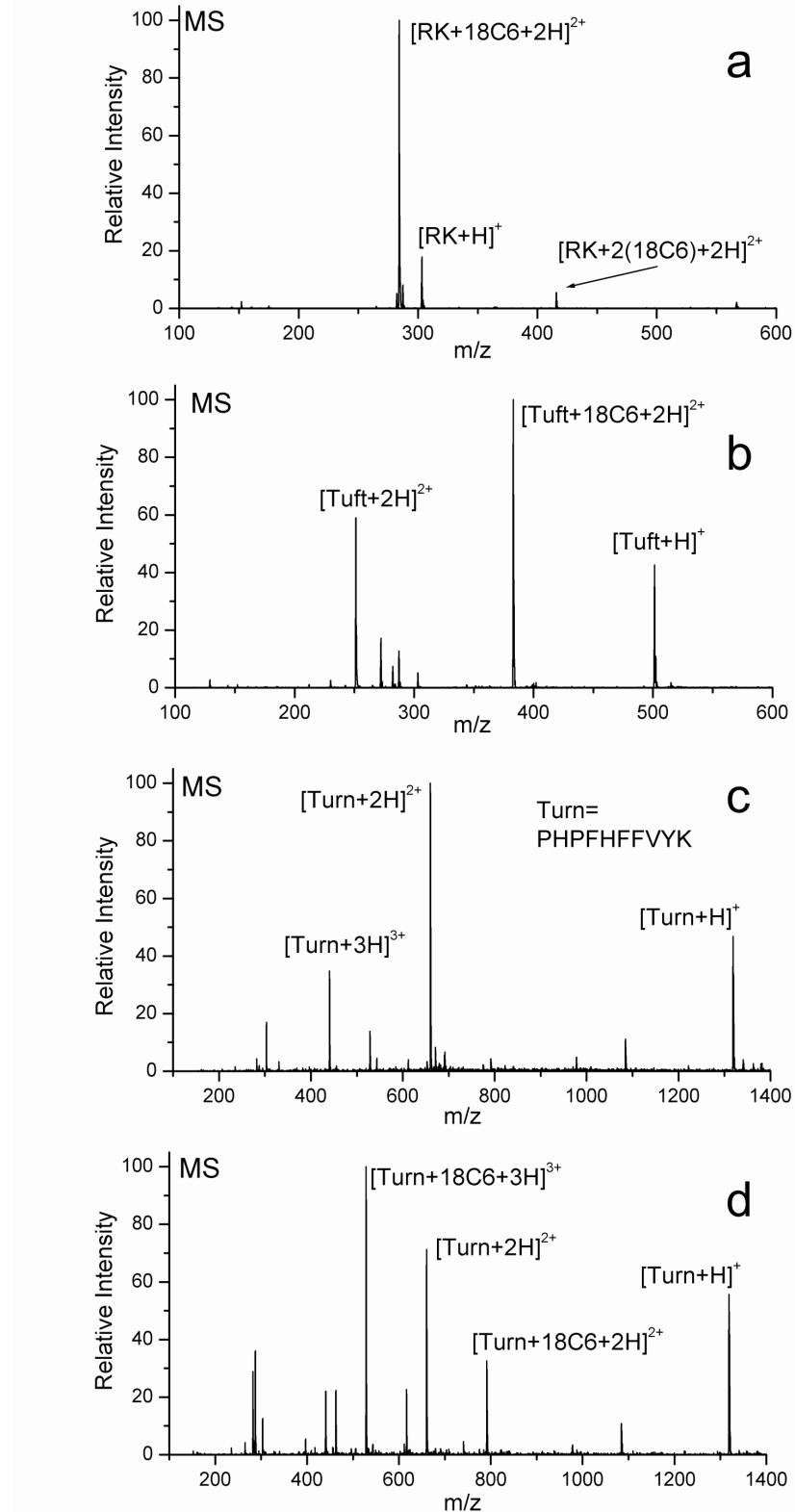


**Figure 7.4** Caption on following page.

**Figure 7.4** (a) Mass spectrum of peptide RK with 18C6. (b) Mass spectrum of tuftsin with 18C6. (c) Typical ESI spectrum of Turn, which with the additions of 18C6 (d) mass again shows an increase in charge state. Some competitive binding by histidine is present in the doubly charged cation.

**Large Peptides and Proteins.** It is tempting to infer that the number of lysines in a peptide can be quantified by counting the number of 18C6 ethers attached to the most abundant adduct. This approach will often work. However, there are several caveats that can make this determination very difficult for a peptide of unknown sequence. For example, molecular conformation may prevent 18C6 from attaching to buried or sterically hindered lysine residues. Cytochrome-c has 19 lysine residues, but attaches a maximum of four 18C6 ethers at room temperature (Table 7.3). This is less than the eleven surface exposed lysines of the folded cytochrome-c. Interestingly, however, there are only four exposed lysines (the maximum number of 18C6 ethers attached to any charge state of cytochrome-c) which are not involved in salt bridges. When cytochrome-c is denatured in solution by heating to 80°C in the presence of 18C6 and then cooled to room temperature, up to eleven crown ethers attach (Table 7.4). 18C6 appears to prevent the refolding of cytochrome-c since nearly identical spectra were obtained when the same solution was electrosprayed two days later.

**Table 7.3 18C6 Adduct Distribution with  
Horse Heart Cytochrome-C at 20 °C**

Charge State	Maximum # of 18C6 Adducts	# of 18C6 in Most Abundant Peak
19	4	4
18	4	3
17	3	3
16	4	1
15	4	1
14	4	1
13	3	1
12	4	1
11	4	1
10	3	1
9	2	1
8	-	-
7	-	-

**Table 7.4 18C6 Adduct Distribution with  
Horse Heart Cytochrome-C heated to 80 °C  
for One Minute and Cooled to 20 °C.**

Charge State	Maximum # of 18C6 Adducts	# of 18C6 in Most Abundant Peak
19	9	9
18	10	10
17	9	9
16	11	9
15	9	8
14	11	10
13	7	7
12	7	6
11	6	5
10	5	3
9	-	-
8	-	-
7	-	-

As noted above, 18C6 can dramatically alter the charge state and abundance of ions observed by ESI. In proteins, this effect is most dramatic where arginine is the primary charge carrier. For example, in Figure 7.5a, BPTI (Bovine pancreatic trypsin inhibitor) shows a dramatic shift in charge state distribution when compared to cytochrome-c (Figure 7.5b). BPTI has 6 arginines and 4 lysines, whereas cytochrome-c has only 2 arginines with 19 lysines. For BPTI, the addition of 18C6 enables the lysine residues to retain available protons in the presence of the more basic arginine residues. In the case of cytochrome-c, most of the exposed lysine residues are already charged and the addition of 18C6 does not greatly affect the charge state distribution.

For proteins, the task of lysine quantification is probably impossible. However the preliminary results presented here are sufficiently intriguing to warrant more detailed studies of a larger number of proteins by varying conditions to effect protein unfolding in the presence of 18C6.

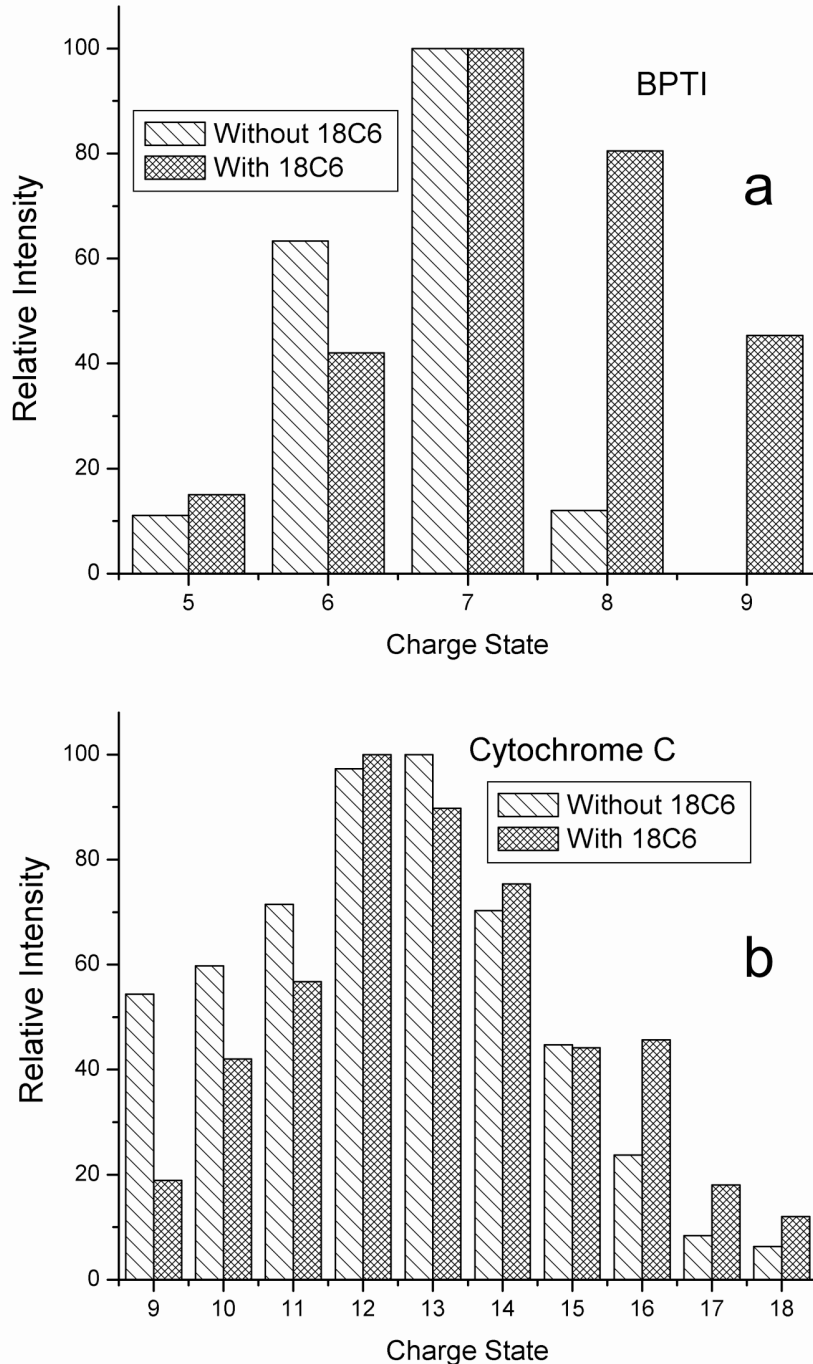


**Figure 7.5** (a) Charge state distribution of BPTI showing the effect of adding 18C6. (b) Cytochrome c taken from horse heart shows less charge stabilization, probably due to fewer arginine residues and the inaccessibility of lysine residues in surface salt bridges.

**Charge Stabilization and Increased Ion Abundance.** The maximum charge state for a peptide produced by ESI is determined by a variety of factors including pH, functional group proton affinities, and solvent. The addition of 18C6 leads to an increase in the charge state for most molecular species. The calculated and experimental proton affinities for the various charge states of several molecules are shown in Table 7.2. Based on these proton affinities,  $[KKKK+3H]^{3+}$  should be the highest charge state produced for KKKK, because the proton affinity of methanol is higher than that for  $[KKKK+3H]^{3+}$ . This prediction is in agreement with the experimental results found in Figure 7.3c and other theoretical approaches predicting the maximum charge state produced with ESI.<sup>18,19</sup> With the addition of 18C6, the +4 charge state is not only observed, but it represents the most abundant ion in the spectrum.

There are essentially two competing processes that control ion evaporation in a highly charged droplet. Coulombic repulsion (or the electric field due to excess charge) drives the charges near the surface of the droplet, while the free energy of solvation retains the charges within the solvent. As a droplet shrinks due to normal evaporation the coulombic repulsion between molecules of like charge increases. Rayleigh fissioning will lead to smaller droplets.<sup>20</sup> Recently experiments in our labs confirmed that when droplets undergo Rayleigh fissioning, a methanol droplet releases 15-20% of the charge with little accompanying loss of solvent.<sup>21</sup> The resulting offspring droplets are very highly charged, and ion evaporation is postulated to occur in these very small droplets when coulombic repulsion overcomes the free energy of solvation for a particular ion. The exact nature of this event is unclear.

It has been shown previously by studies of nonpolar analytes that relative ion abundance can be increased by increasing the surface activity of an analyte.<sup>22,23</sup> 18C6 adducts also lead to enhanced ion yields in electrospray ionization. 18C6 excludes solvent from the ion and is often used as a phase transfer catalyst suggesting that the resulting complexes are neither hydrophilic nor hydrophobic. The surface activity of an ion complexed with 18C6 is increased by reducing both the polar nature of the ion and the magnitude of the free energy of solvation. The Born equation serves as a first approximation for the free energy of solvation.<sup>24</sup> In a semi-quantitative approximation, the calculated molecular volumes listed in Table 7.2 are taken to be spherical. The corresponding radius is used in the Born equation. Using this approach, the addition of 18C6 reduces the free energy of solvation for NH<sub>4</sub><sup>+</sup> by 204 kJ/mol. Based on this result, it is expected that [KKKK+4(18C6)+4H]<sup>4+</sup> would be very easily desolvated in comparison with [KKKK+4H]<sup>4+</sup>. The coulombic repulsion within the droplet and low magnitude of the free energy of solvation would increase the surface activity and concomitantly the ion abundance of the 18C6 adduct.

The preferential charging and desolvation of molecular species with 18C6 attached has an interesting consequence. In an experiment with KKKK, the concentration of 18C6 was varied from slightly below the stoichiometric ratio for the number of available binding sights (i.e. the number of lysines) to one 18C6 for four lysines. As seen in Figure 7.6, the spectrum changes very little despite the lowering of the 18C6/KKKK ratio well below the stoichiometric equivalency. The fact that the [KKKK+4(18C6)+4H]<sup>4+</sup> peak dominates the spectrum shown in Figure 7.6b suggests that solution phase concentrations are clearly not represented in the gas phase ion abundance of these species.

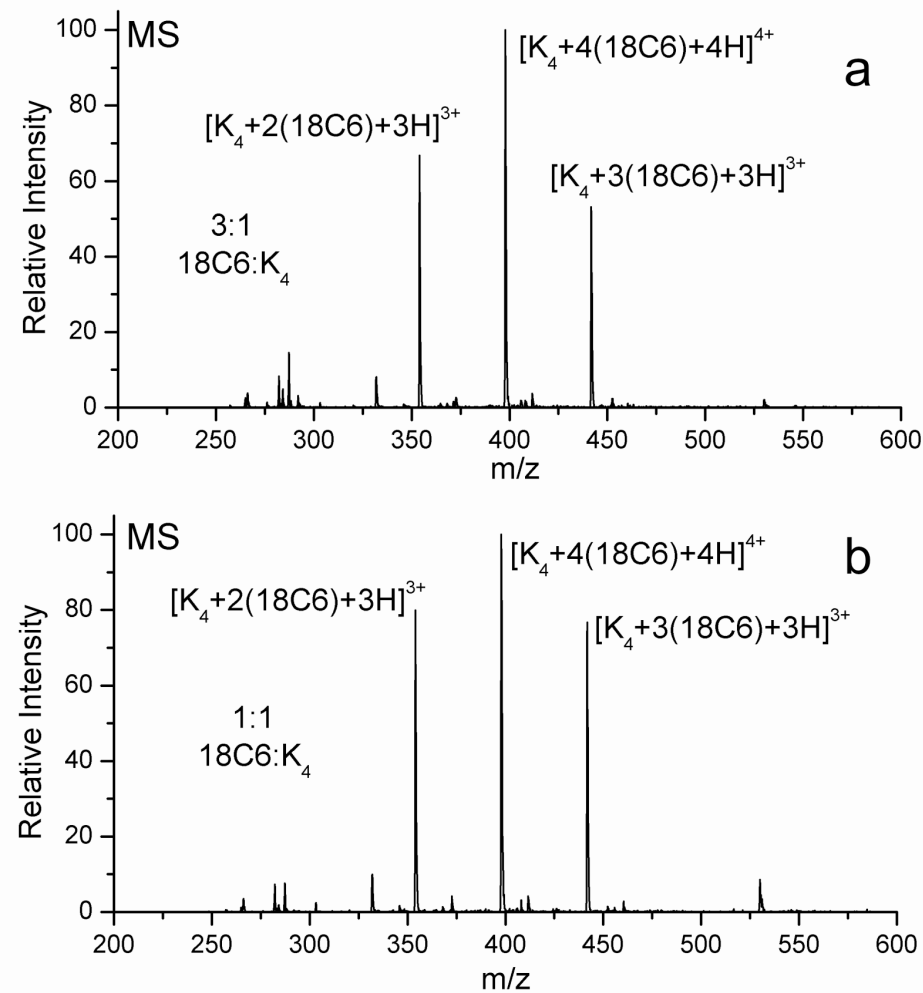


**Figure 7.6** Effect of concentration on 18C6 binding. (a) 3:1, (b) 1:1 (18C6 to KKKK) concentrations respectively. The solution phase concentrations are not accurately reflected in the gas phase distribution.

Only a very small fraction of the analyte introduced via ESI ever reaches the detector. In fact, for a typical ESI methanol droplet with a diameter of 15 microns there are approximately  $1.5 \times 10^6$  charges when the droplet is at the Rayleigh limit.<sup>21</sup> Using these numbers, there are approximately 35 molecules/charge in a droplet that was formed from a 50  $\mu\text{M}$  solution (this should be regarded as a lower limit for the analyte/charge ratio because it neglects evaporation that may have already concentrated the solution). Under these conditions, there are far more molecules of analyte in an ESI droplet than there are charges to allow for their detection. Taking this into account, if the rate at which an ion is expelled from the droplet is increased, then the ion abundance will be greatly increased. The lack of sufficient charge introduces a time dependence on the ion abundance where those ions that are “evaporated” first will be the most abundant.

#### 7.4 Conclusion

Lysine forms a stable salt-bridge complex with 18C6 complexed to the N-terminus. In peptides, however, the side chain of lysine is found to be the preferred binding site. 18C6 can even sequester charge on several adjacent lysines as demonstrated by the abundance of  $[\text{KKKK}+4(18\text{C6})+4\text{H}]^{4+}$  (structure 7.8, Figure 7.3d). Lysine residues can usually be quantified in small peptides by counting the number of 18C6 ethers attached to the peptide in the most abundant peak of the spectrum. In larger peptides and proteins, 18C6 is sensitive to and may be used to detect changes in conformation. It is clear that 18C6 can prevent the refolding of a denatured protein for an extended period of time. Competitive complexation by the side chains of histidine and arginine is low. The binding of 18C6 is found to dramatically alter the ion abundance and the charge state

distribution of most species to which it attaches. This charge stabilization is useful because it allows for the facile detection of species that are normally difficult to detect with ESI, but it also complicates the quantification of lysine through molecular recognition.

<sup>18</sup>C6 will form a stable adduct to primary amines in both solution and the gas phase. This complexation reduces the magnitude of the free energy of solvation for the ions and facilitates their removal to the gas phase. The result is that the charge state distribution and ion abundance of the peptide are affected. With further research in this area, it may be possible to expand the capabilities of ESI by tailoring molecular interactions that allow for the detection of others species that are difficult to electrospray. In the case demonstrated here, the charge state and ion abundance are increased primarily for lysine rich molecules; however, there is no limitation that precludes this principle from operating in other systems. Further experiments may lead to fine-tuned reagents which are highly selective for binding to specific residues.

## 7.5 References

---

- <sup>1</sup> Hiraoka, M. *Crown Compounds: their characteristics and applications* Elsevier Scientific Publishing Company: New York, 1982.
- <sup>2</sup> Schalley, C. A. *Int. J. Mass Spec.* **2000**, *194*, 11-39.
- <sup>3</sup> Pope, R. M.; Shen, N.; Hofstadler, S. A.; Dearden, D. V. *Int. J. Mass Spec. Ion Proc.* **1998**, *175*, 179-186. Cunniff, J. B.; Vouros, P. *J. Am. Soc. Mass Spectrom.* **1995**, *6*, 1175-1182.
- <sup>4</sup> Rudiger, V.; Schneider, H. J.; Solov'ev, V. P.; Kazachenko, V. P.; Raevsky, O. A. *Eur. J. Org. Chem.* **1999**, 1847-1856.
- <sup>5</sup> *Comprehensive Supramolecular Chemistry*, vol. 1 (Ed.:G. W. Gokel), Pergamon/Elsevier: Oxford, 1996.
- <sup>6</sup> More, M. B.; Ray, D.; Armentrout, P. B. *J. Am. Chem. Soc.* **1999**, *121*, 417-423.
- <sup>7</sup> Williamson, B. L.; Creaser, C. S. *Int. J. Mass Spec.* **1999**, *188*, 53-61.
- <sup>8</sup> Maleknia, S.; Brodbelt, J. *J. Am. Chem. Soc.* **1993**, *115*, 2837-2843.
- <sup>9</sup> Meot-ner, M. *J. Am. Chem. Soc.* **1983**, *105*, 4912-4915.
- <sup>10</sup> (a) He, Z. M.; Zhang, Z. D. *J. Protein Chem.* **1999**, *18*, 557-564. (b) Vila, J. A.; Ripoll, D. R.; Villegas, M. E.; Vorobjev, Y. N.; Scheraga, H. A. *BioPhys. J.* **1998**, *75*, 2637-2646.
- <sup>11</sup> Lee, S. -W.; Lee, H. -N.; Kim, H. S.; Beauchamp, J. L. *J. Am. Chem. Soc.* **1998**, *120*, 5800-5805.
- <sup>12</sup> Fenn, J.; Rosell, J.; Nohmi, T.; Shen, S.; Banks, F. *Biochemical and Biotechnological Applications of Electrospray Ionization Mass Spectrometry* **1996**, *619*, 60-80.

---

<sup>13</sup> (a) Iribarne, J. V.; Thomson, B. A. *J. Chem. Phys.* **1976**, *64*, 2287. (b) Thomson, B. A.; Iribarne, J. V. *J. Chem. Phys.* **1979**, *71*, 4451.

<sup>14</sup> Mayo, S. L.; Olafson, B. D.; Goddard, W. A. *J. Phys. Chem.* **1990**, *94*, 8897-8909.

<sup>15</sup> Campbell, S.; Beauchamp, J. L.; Rempe M.; Lichtenberger D. L. *Int. J. Mass Spec.* **1992**, *117*, 1-3.

<sup>16</sup> E. P. Hunter and S. G. Lias, "Proton Affinity Evaluation" in NIST Chemistry WebBook, NIST Standard Reference Database Number 69, Eds. W.G. Mallard and P.J. Linstrom, February 2000, National Institute of Standards and Technology, Gaithersburg MD, 20899 (<http://webbook.nist.gov>)

<sup>17</sup> Kulikov, O. V.; Krestov, G. A. *Pure & Appl. Chem.* **1995**, *67*, 1103-1108.

<sup>18</sup> Wong, S. F.; Meng, C. K.; Fenn, J. B. *J. Phys. Chem.* **1988**, *92*, 546-550.

<sup>19</sup> (a) Schnier, P. D.; Gross, D. S.; Williams, E. R. *J. Am. Soc. Mass Spectrom.* **1995**, *6*, 1086-1097. (b) Schnier, P.D.; Price, W. D.; Williams, E. R. *J. Am. Soc. Mass Spectrom.* **1996**, *7*, 972-976.

<sup>20</sup> Lord Rayleigh *Proc. Roy. Soc.* **1882**, *14*, 184-186.

<sup>21</sup> Smith, J. N.; Flagan, R. C.; Beauchamp, J. L. *J. Phys. Chem. A* **2002**, *106*, 9957-9967.

<sup>22</sup> Cech, N. B.; Enke, C. G. *Anal. Chem.* **2000**, *72*(13), 2717-2723.

<sup>23</sup> Tang, L.; Kebarle, P. *Anal. Chem.* **1993**, *65*, 3654-3668.

<sup>24</sup> Born, M. *Phys. Z.* **1920**, *1*, 45.